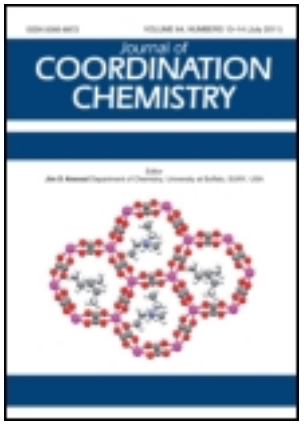


Journal of Coordination Chemistry
Publication details, including instructions for authors and subscription information:
http://www.tandfonline.com/loi/gcoo20

# Surfactant-assisted low-temperature thermal decomposition route to spherical NiO nanoparticles

Chira R. Bhattacharjee [a], Debraj Dhar Purkayastha [a] & Jitu Ranjan Chetia [b]

[a] Department of Chemistry, Assam University, Silchar 788 011, Assam, India

[b] Department of Chemistry, Dibrugarh University, Dibrugarh 786 004, Assam, India

Published online: 06 Dec 2011.

To cite this article: Chira R. Bhattacharjee, Debraj Dhar Purkayastha & Jitu Ranjan Chetia (2011) Surfactant-assisted low-temperature thermal decomposition route to spherical NiO nanoparticles, Journal of Coordination Chemistry, 64:24, 4434-4442, DOI: 10.1080/00958972.2011.640396

To link to this article: http://dx.doi.org/10.1080/00958972.2011.640396

*Journal of Coordination Chemistry*
Vol. 64, No. 24, 20 December 2011, 4434–4442



# Surfactant-assisted low-temperature thermal decomposition route to spherical NiO nanoparticles

CHIRA R. BHATTACHARJEE*†, DEBRAJ DHAR PURKAYASTHA† and JITU RANJAN CHETIA‡

†Department of Chemistry, Assam University, Silchar 788 011, Assam, India
‡Department of Chemistry, Dibrugarh University, Dibrugarh 786 004, Assam, India

(*Received 1 September 2011; in final form 4 November 2011*)

Thermal decomposition has been employed to access spherical nickel oxide (NiO) nanoparticles from a new precursor, nickel-salicylate, $[Ni(C_7H_5O_3)_2(H_2O)_4]$. Surfactants, triphenylphosphine ($(C_6H_5)_3P$), and oleylamine ($C_{18}H_{35}NH_2$) were added to control the particle size. The products were characterized by X-ray diffraction, transmission electron microscopy (TEM), Fourier transform infrared spectroscopy, and thermogravimetric analysis. TEM images showed particles nearly spherical having sizes 5–15 nm. The magnetism of NiO nanoparticles was studied with a vibrating sample magnetometer. Due to smaller particle size and increased surface uncompensated spins, a superparamagnetic behavior is observed. The synthetic process is simple and affords high-purity material at a relatively lower calcination temperature.

*Keywords*: Nanoparticles; NiO; Thermal decomposition; Superparamagnetic



## 1. Introduction

Science and technology of nanostructured metal oxides have captivated scientists during the last couple of decades. Particles of metal oxides from 1 to 100 nm can serve as good absorbents, carriers, and catalysts. Nickel oxide (NiO) is one of the most promising metal oxides for various applications. Besides fundamental research interests, nano-NiO, a p-type semiconductor, with a stable wide band gap (3.4–4.0 eV) [1] is used in alkaline batteries, gas sensors, electrochemical capacitors, smart windows, biomedicine, drug delivery, and magnetic bar codes [2–8]. The structural properties of nano metal oxides are intricately related to preparative techniques. Several methods such as thermal decomposition [9], electrodeposition [10], sputtering [11], homogeneous precipitation [12, 13], and sol–gel [14, 15] have been documented for the synthesis of nano-NiO. The preparation of well-crystallized oxide nanoparticles generally requires high-temperature treatment (typically above 1000°C), leading to irreversible growth and coalescence of starting particles [16]. Delicate control of synthetic conditions can afford ultra fine powders with narrow particle size distribution and enhanced material performance. Using different amines and surfactants, varying concentration, and

*Corresponding author. Email: crbhattacharjee@rediffmail.com


ISSN 0095-8972 print/ISSN 1029-0389 online © 2011 Taylor & Francis
http://dx.doi.org/10.1080/00958972.2011.640396

composition of solvents, Wu *et al*. [17] obtained nano-NiO particles possessing different morphologies, sizes, and shapes. Microemulsion route using cationic surfactant [18], chemical precipitation from nickel nitrate and urea [19] are also on record. Effects of anions such as nitrate, chloride, sulfate, or acetate on the sizes and morphology of nano-NiO and magnetism has been studied recently [20]. Li *et al*. [21] synthesized NiO nanoparticles using nickel nitrate and urea as starting materials and evaluated the catalytic properties of the material in pyrolyzing cellulose. Of all such methods, thermal decomposition method is a preferred process to access nano-NiO of different sizes and shapes, as it is simple, cost-effective, and affords high purity materials [22]. Although thermal decomposition of many metal salicylates [23] and nickel salicylate [23–25], in particular, has been investigated, no previous studies addressed the synthesis of metal oxide nanoparticles from such precursors. Addressing the challenge we intended to devise the synthesis of spherical NiO nanoparticles by thermal decomposition of nickel-salicylate complex, $[Ni(C_7H_5O_3)_2(H_2O)_4]$, in the presence of surfactants triphenylphosphine (TPP) and oleylamine as stabilizers.



## 2. Experimental

### 2.1. *Materials*

The precursor $[Ni(C_7H_5O_3)_2(H_2O)_4]$ was prepared according to the literature procedure [25] with little modification. Oleylamine, TPP, *n*-hexane, and ethanol were purchased from Aldrich and used as received.

### 2.2. *Techniques*

Powder X-ray diffraction (XRD) measurements were carried out on a Bruker AXS D8-Advance powder X-ray diffractometer with Cu-K$\alpha$ radiation ($\lambda = 1.5418$ Å) with a scan speed $2^\circ\,min^{-1}$. FT-IR spectra were recorded on a Shimadzu Varian 4300 spectrometer with KBr pellets. Elemental analyses (C, H, and N) were performed on a Heraeus Vario EL III Carlo Erba 1108 elemental analyzer. Nickel content was analyzed by atomic absorption spectroscopy (AAS) using Perkin Elmer ANA-Analyst 200 model equipment. Thermogravimetric analysis (TGA) was performed on a Perkin Elmer Pyris Diamond thermal analyzer maintaining a flow rate of $20\,mL\,min^{-1}$ and a heating rate of $10^\circ C\,min^{-1}$ in air. Transmission electron microscopy (TEM) images were obtained on a Jeol, 9JSM-100CX TEM with an accelerating voltage of 100 kV. The sample powders were dispersed in *n*-hexane under sonication and TEM grids were prepared using a few drops of the dispersion followed by drying in air. Magnetism of the material was studied using a Vibrating Sample Magnetometer (VSM, Lakeshore Model 7410) at 300 K.

### 2.3. *Synthesis of* $[Ni(C_7H_5O_3)_2(H_2O)_4]$

$NiCl_2 \cdot 6H_2O$ (1.1885 g, 5 mmol) and salicylic acid (1.3812 g, 10 mmol) were dissolved in distilled water separately and mixed in a conical flask and stirred for 1 h. The pH of the

resultant solution was maintained at ~8 by the addition of 5% aqueous KOH solution and further stirred for 2 h. The green precipitate thus obtained was filtered, washed, and dried. The product was characterized by FT-IR, elemental analyses, and TGA. Anal. Calcd for $[Ni(C_7H_5O_3)_2(H_2O)_4]$ (%): C, 41.51; H, 4.45; Ni, 14.50. Found (%): C, 41.56; H, 4.49; Ni, 14.55. FT-IR ($\nu_{max}$, $cm^{-1}$, KBr): 3385 ($\nu_{O-H}$), 1600 ($\delta_{HOH}$), 1570 ($\nu_{a(C-O)}$), 1400 ($\nu_{s(C-O)}$), 1235 ($\delta_{COH}$).

### 2.4. *Synthesis of NiO nanoparticles*

$[Ni(C_7H_5O_3)_2(H_2O)_4]$ (0.6 g) was taken in a round-bottomed flask and 5 mL of oleylamine was added to it and heated for 1 h at 140°C on an oil bath to get $[Ni(C_7H_5O_3)_2(H_2O)_2(oleylamine)_2]$ complex. TPP (5 g) was then added to the resultant solution and temperature was raised to 240°C. The initial green color of the solution changed to black. The black solution thus obtained was aged at 240°C for 1 h and cooled to room temperature. The black solids were precipitated by adding excess ethanol to the reaction solution. The product is washed with ethanol several times. The solids could be easily re-dispersed in nonpolar organic solvents like *n*-hexane or toluene.



## 3. Results and discussion

The synthesis described herein is a modified version of the procedure developed by Hyeon and others for the synthesis of metal and oxide nanocrystals that utilizes thermal decomposition of transition metal complexes [22, 26]. In current synthesis (scheme 1), NiO nanoparticles were prepared by the thermal decomposition of a nickel-salicylate complex, $[Ni(C_7H_5O_3)_2(H_2O)_4]$ as precursor in the presence of oleylamine and TPP. Oleylamine with its long hydrocarbon tail is considered to replace two non-hydrogen-bonded labile water molecules from the coordination sphere of nickel(II) forming $[Ni(C_7H_5O_3)_2(H_2O)_2(oleylamine)_2]$ (scheme 1). A rather similar synthetic philosophy has recently been exploited for the preparation of nano-NiO from nickel oxalate complex, $[Ni(C_2O_4)(H_2O)_4]$ [22]. Pertinent here is to mention that a calcination temperature lower than 240°C did not afford any NiO nanoparticles. In fact, the green reaction solution did not undergo any change until 240°C. Transformation to a blackish

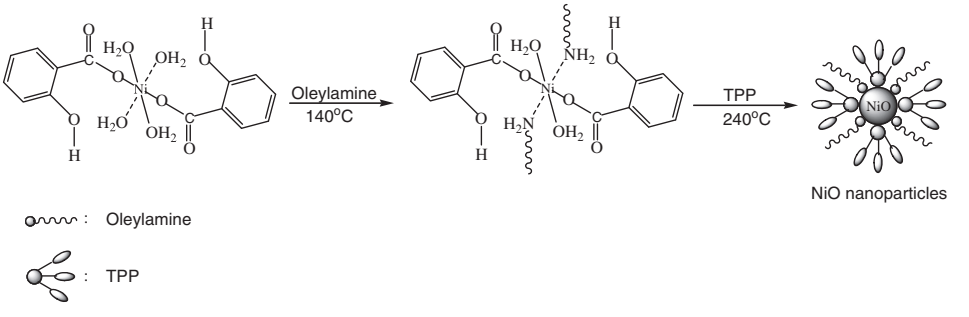


Scheme 1. Illustration of the formation of NiO nanoparticles.

solution occurred only at 240°C while temperature above 240°C led to particles of bigger size. Further, under similar experimental conditions, when only oleylamine (no TPP) was used, highly agglomerated NiO particles were formed while with TPP alone (no oleylamine) no NiO could be obtained (table 1). Thus, it is evident that oleylamine and TPP together played a crucial role in the synthesis of low-dimensional NiO nanoparticles at a relatively low temperature. As the surface area of metal nanoparticles is related to their masses, they possess an excess surface free energy comparable to the lattice energy rendering the particles thermodynamically unstable. Protective or capping agents outweigh the attractive van der Waals forces by repulsive steric interaction. It is believed that the sterically demanding surfactant molecules aid in achieving greater interparticle separation [27].

The as-synthesized NiO nanoparticles were characterized by XRD, TEM, FT-IR, and VSM studies. The C, H, and N microanalysis as well as AAS analysis of the nickel content of the metal-salicylate precursor and the as-obtained NiO nanomaterial were carried out to confirm the compositions. Somewhat less nickel content is expected for NiO only and the occurrence of non-stoichiometric proportion of C, H, and N in the sample further affirms the presence of some surfactant molecules coating the nanoparticles. The TGA (figure 1) of the as-prepared precursor complex shows three distinct weight loss steps. The first step, in the temperature range 40–150°C, involves the loss of water yielding the anhydrous material. Such wide temperature range for loss of

Table 1. Calcination of $[Ni(C_7H_5O_3)_2(H_2O)_4]$ under different experimental conditions.

| Sample | Surfactants | Calcination temperature (°C) | Time | Products (size) |
|---|---|---|---|---|
| 1 | None | 450 | 2 h | Bulk NiO |
| 2 | Oleylamine | 240 | 2 h | Agglomerated NiO |
| 3 | TPP | 240 | 2 h | No products |
| 4 | Oleylamine + TPP | 240 | 2 h | NiO (5–15 nm) |

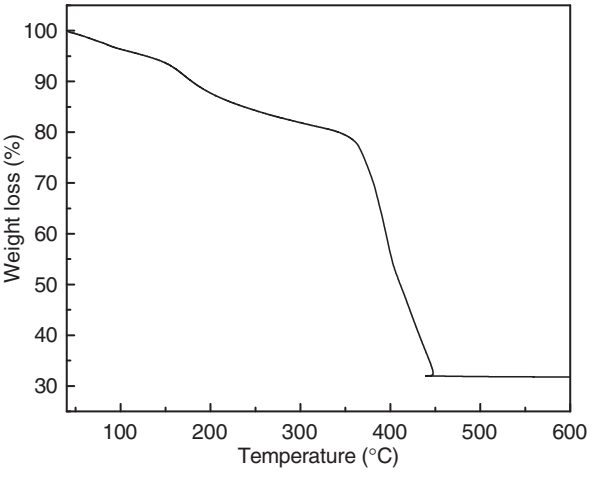


Figure 1. TGA curve of $[Ni(C_7H_5O_3)_2(H_2O)_4]$.

four water molecules alone clearly suggest that the four water molecules are not of the same type. A previous report [25] which dealt with structural characterization of nickel-salicylate complex shows that all four water molecules are coordinated, of which two are further H-bonded to each monodentate salicylate. In the present case the nickel-salicylate complex on being treated with oleylamine leads to the replacement of only two water molecules, presumably the non-H-bonded ones (scheme 1), further confirming the nature of water in the nickel-salicylate complex. The second step in the temperature range 150–340°C is due to the loss of one salicylate, and the third and final step in the temperature range 340–450°C is oxidation of this intermediate to the metal-oxide.

As evident from TGA analysis, the final weight loss step which corresponds to the loss of one salicylate leading to bulk NiO was found to occur at 450°C, however, use of capping ligands, oleylamine, and TPP lowered the decomposition temperature substantially, affording nano-NiO particles.

The proper selection of metal precursor and the method of synthesis is crucial to the preparation of nano metal oxides. Thermal treatment of different precursors can result in variation of particle sizes of nanocrystalline NiO depending on the temperature. For instance, surfactant-unassisted direct calcination of nickel dimethylglyoximate [28], nickel oxalate dihydrate [29], and nickel-*o*-phthalate [30] at different temperatures lead to NiO of different particle sizes. Calcination of nickel dimethylglyoximate at 500°C resulted in nanocrystalline NiO of mean particle size 35 nm, nickel oxalate dihydrate afforded NiO nanoparticles of mean size 30 nm at 450°C, while nickel-*o*-phthalate produced NiO of mean particle size 15 nm at 500°C. Not only the calcination temperatures are higher in these methods, but the sizes of the nanoparticles obtained are also larger. Nano-NiO of particle sizes $<10$ nm are difficult to obtain by these procedures. In this context a particle size of $\sim$6 nm obtained for NiO at a relatively low temperature of 240°C is a redeeming feature of this work.

FT-IR spectroscopy was used to discern the nature of the surface-coordinating organic capping groups that facilitate dispersion of the nanoparticles in organic solvents. Figure 2 shows the FT-IR spectrum of NiO nanoparticles. The peak at

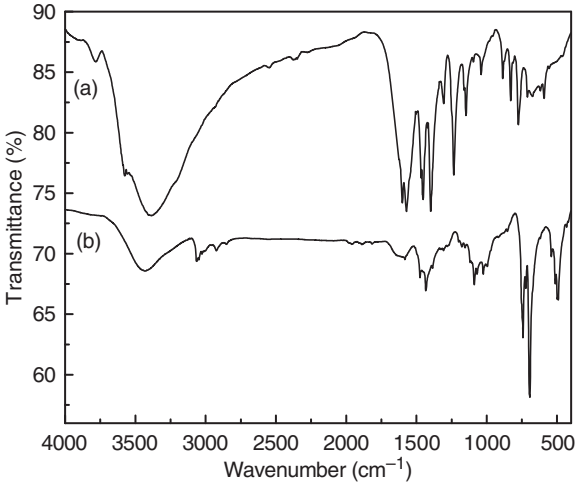


Figure 2. FT-IR spectra of (a) $[Ni(C_7H_5O_3)_2(H_2O)_4]$ and (b) NiO nanoparticles.

490 $cm^{-1}$ (curve b), attributable to Ni–O stretching vibration furnished clear evidence for the presence of crystalline NiO. A broad peak at ~3435 $cm^{-1}$ (curve b) indicates the presence of water. As the material was exposed to ambient conditions after calcination, some moisture was adsorbed on the external surface probably during spectrum recording. The H–O–H bending vibration appeared at ~1630 $cm^{-1}$ (curve b). The spectrum contains a number of weak peaks between 1000–1400 $cm^{-1}$ and 2800–3000 $cm^{-1}$ which arise due to symmetric and asymmetric stretching vibrations of $-CH_2$, terminal $-CH_3$ and =CH of oleylamine ($C_{18}H_{35}NH_2$). The material exhibited two weak stretching vibrations at ~2918 and 2845 $cm^{-1}$ assignable to C–H stretch of oleylamine carbon chain. Also, a broad band due to C–N the stretch of oleylamine was observed at ~1150 $cm^{-1}$ (curve b). These results indicate that some oleylamine molecules were adsorbed on the surface of NiO nanoparticles. The sharp peak at ~1435 $cm^{-1}$ (curve b) attributable to the phosphorus-phenyl stretching mode $\nu$(P–Ph) also suggested the occurrence of some TPP in the material.

At 240°C, most surfactant molecules (capping ligands) such as oleylamine and TPP were decomposed. The calcined NiO material was thoroughly washed with ethanol several times to remove any residual surfactant molecules and then subjected to elemental analysis (vide infra) to ascertain the extent of adsorbed surfactant molecules on the as-obtained material. Owing to the presence of the surfactant molecules, the NiO material can easily be dispersed in organic solvents such as *n*-hexane and toluene. Oleylamine serves as both solvent and capping agent for the nanoparticles. The long hydrocarbon chain of oleylamine exerts greater steric hindrance to control the size of metal nanoparticles. It is believed that oleylamine passivates the surface of grown nanoparticles, thus preventing agglomeration [27]. The stabilization of metal nanoparticles with TPP is also well documented in the literature [31, 32]. TPP, a high-boiling point surfactant with three phenyl rings impose greater steric hindrance slowing the rate of agglomeration of the nanoparticles during their growth, producing much smaller particles. Addition of TPP to $[Ni(C_7H_5O_3)_2(H_2O)_2(oleylamine)_2]$ (vide infra) resulted in much smaller particles with uniform size distribution.

### 3.1. *Powder X-ray diffraction study*

The X-ray powder diffraction pattern was recorded at room temperature for the identification of phases exhibited by the synthesized material. Figure 3 shows the XRD pattern of the synthesized material. The product is characterized as NiO (JCPDS file no: 73-1523). The diffraction peaks can be exactly indexed to a cubic structure of NiO with cell constant $a = 4.197$ Å. No characteristic peaks of impurity were observed. The average particle size of NiO was estimated by Debye–Scherrer formula ($d = 0.9\lambda/\beta\cos\theta$) to be 6.2 nm. The diffraction peaks are all quite broad, indicating the nanocrystalline nature of the material.

### 3.2. *TEM*

The morphology and particle size of the synthesized materials were determined by TEM. For preparation of the TEM sample, the powder was dispersed in *n*-hexane *via* ultrasonic equipment. The TEM image (figure 4) of NiO produced under the given experimental conditions exhibited nearly spherical morphology and is well dispersed

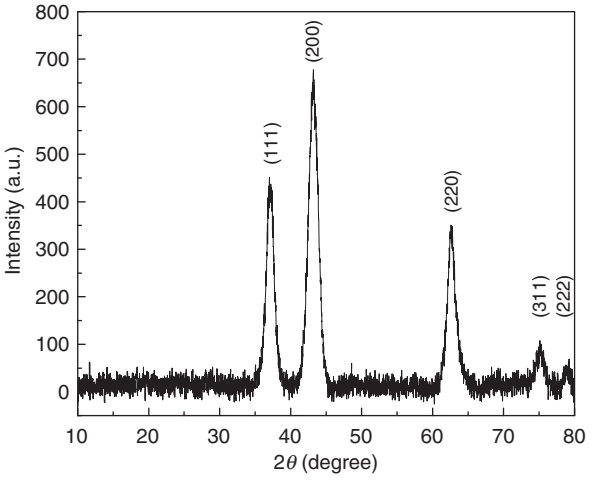


Figure 3. XRD pattern of NiO nanoparticles.

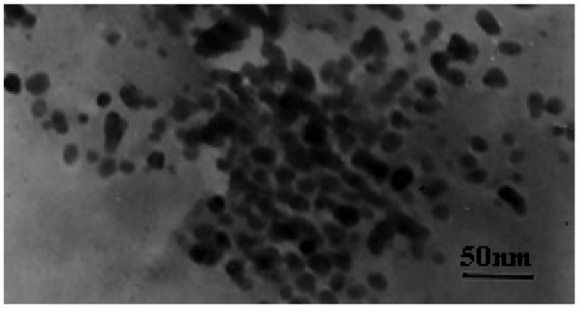


Figure 4. TEM image of NiO nanoparticles.

with no agglomerations. The size of nanoparticles obtained from the XRD pattern are in close agreement with TEM studies which indicated the particle sizes to be 5–15 nm.

### 3.3. *Room temperature magnetic study*

The magnetization *versus* applied magnetic field (M–H) curve of NiO nanoparticles (figure 5) recorded at room temperature shows a hysteresis loop typical of superparamagnetic behavior. Bulk NiO is antiferromagnetic with a Neel temperature of 523 K [33]. Surface effects can dominate the net magnetic behavior for nano-NiO particles. Presence of a large fraction of atoms on the surface possessing uncompensated spins led to the net magnetization [34]. Greater surface spins with low coordination and broken exchange bonds enhance the net magnetization. The spherical nano-NiO prepared in this work possess smaller particle size (~6.2 nm). This increases the surface uncompensated spins, resulting in a superparamagnetic behavior (figure 5).

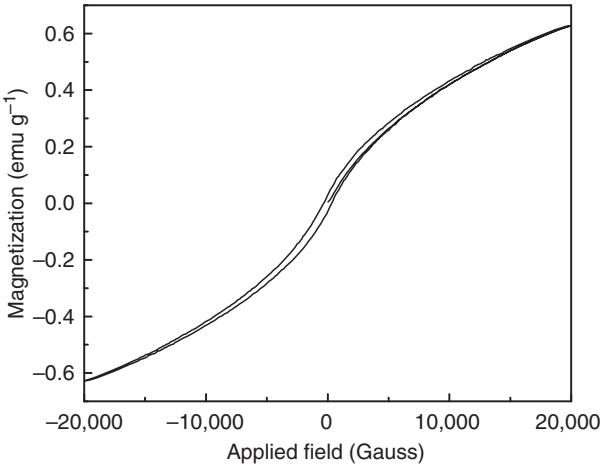


Figure 5. Magnetization ($M$) *vs.* applied field ($H$) plot of NiO nanoparticles at 300 K.



## 4. Conclusion

Spherical NiO nanoparticles of 5–15 nm have been synthesized *via* low-temperature thermal decomposition of a new precursor, $[Ni(C_7H_5O_3)_2(H_2O)_4]$. The role of surfactant stabilizers oleylamine and TPP was vital in controlling the growth of the particles and lowering the calcination temperature. The XRD pattern showed phase pure cubic NiO. The current method employed is an inexpensive reproducible process with potential for scale-up. The methodology can be readily extended for the synthesis of other nano metal oxides.

## Acknowledgments

Authors are thankful to SAIF, NEHU, Shillong, and CIF, IIT, Guwahati, for providing instrumental facilities. D.D. Purkayastha thanks University Grants Commission, Government of India, for providing grants under Research Fellowship Scheme for Meritorious Students (RFSMS).

## References

[1] H. Yang, Q. Tao, X. Zhang, A. Tang, J. Ouyang. *J. Alloys Compd.*, **459**, 98 (2008).
[2] J. Bahadur, D. Sen, S. Mazumder, S. Ramanathan. *J. Solid State Chem.*, **181**, 1227 (2008).
[3] I. Hotovy, J. Huran, L. Spiess, S. Hascik, V. Rehacek. *Sens. Actuators B*, **57**, 147 (1999).
[4] T. Nathan, A. Aziz, A.F. Noor, S.R.S. Prabaharan. *J. Solid State Electrochem.*, **12**, 1003 (2008).
[5] C.G. Granqvist (Ed.). *Handbook of Inorganic Electrochromic Materials*, Elsevier, Amsterdam (1995).
[6] Q.A. Pankhurst, J. Connolly, S.K. Jones, J. Dobson. *J. Phys. D: Appl. Phys.*, **36**, R167 (2003).
[7] C. Sun, J.S. Lee, M. Zhang. *Adv. Drug Delivery Rev.*, **60**, 1252 (2008).
[8] J.H. Lee, J.H. Wu, H.L. Liu, J.U. Cho, M.K. Cho, B.H. An, J.H. Min, S.J. Noh, Y.K. Kim. *Angew. Chem. Int. Ed.*, **46**, 3663 (2007).

[9] C.S. Carney, C.J. Gump, A.W. Weimer. *Mater. Sci. Eng. A*, **431**, 1 (2006).
[10] C. Natarajan, H. Matsumoto, G. Nogami. *J. Electrochem. Soc.*, **144**, 121 (1997).
[11] K. Yoshimura, T. Miki, S. Tanemura. *Jpn. J. Appl. Phys.*, **34**, 2440 (1995).
[12] K.C. Liu, M.A. Anderson. *J. Electrochem. Soc.*, **143**, 124 (1996).
[13] M.S. Wu, H.H. Hsieh. *Electrochim. Acta*, **53**, 3427 (2008).
[14] A. Surca, B. Orel, B. Pihlar, P. Bukovec. *J. Electroanal. Chem.*, **408**, 83 (1996).
[15] S.D. Tiwari, K.P. Rajeev. *Thin Solid Films*, **505**, 113 (2006).
[16] G. Mialon, M. Gohin, T. Gacoin, J.P. Boilot. *ACS Nano.*, **2**, 2505 (2008).
[17] Y. Wu, Y. He, T. Wu, T. Chen, W. Weng, H. Wan. *Mater. Lett.*, **61**, 2679 (2007).
[18] D.Y. Han, Y.H. Yang, C.B. Shen, X. Zhou, F.H. Wang. *Powder Tech.*, **147**, 113 (2004).
[19] X. Xin, Z. Lu, B. Zhou, X. Huang, R. Zhu, X. Sha, Y. Zhang, W. Su. *J. Alloys Compd.*, **427**, 251 (2007).
[20] V. Ranga Rao Pulimi, P. Jeevanandam. *J. Magn. Magn. Mater.*, **321**, 2556 (2009).
[21] J.-F. Li, B. Xiao, L.-J. Du, R. Yan, T.D. Liang. *J. Fuel Chem. Technol.*, **36**, 42 (2008).
[22] M. Salavati-Niasari, N. Mir, F. Davar. *Polyhedron*, **28**, 1111 (2009).
[23] K. Rissanen, J. Valkonen, P. Kokkonen, M. Leskela. *Acta Chem. Scand.*, **A41**, 299 (1987).
[24] K. Kishore, R. Nagarajan. *Thermochim. Acta*, **67**, 351 (1983).
[25] W.J. Long, Y.L. Jie, Y.Y. Yong, S.J. Tang, Z.K. Li. *J. Wuhan Univ. (Natural Science Ed.)*, **8**, 853 (2003).
[26] J. Park, E. Kang, S.U. Son, H.M. Park, M.K. Lee, J. Kim, K.W. Kim, H.J. Noh, J.H. Park, C.J. Bae, J.G. Park, T. Hyeon. *Adv. Mater.*, **17**, 429 (2005).
[27] B. Corain, G. Schmid, N. Toshima (Eds). *Catalysis and Materials Science: The Issue of Size Control*, p. 21, Elsevier Publishers, Oxford (2008).
[28] X. Li, X. Zhang, Z. Li, Y. Qian. *Solid State Commun.*, **137**, 581 (2006).
[29] T. Ahmad, K.V. Ramanujachary, S.E. Lofland, A.K. Ganguli. *Solid State Sci.*, **8**, 425 (2006).
[30] M. Salavati-Niasari, F. Mohandes, F. Davar, M. Mazaheri, M. Monemzadeh, N. Yavarinia. *Inorg. Chim. Acta*, **362**, 3691 (2009).
[31] H.T. Yang, Y.K. Su, C.M. Shen, T.Z. Yang, H.J. Gao. *Surf. Interf. Anal.*, **36**, 155 (2004).
[32] M. Salavati-Niasari, F. Davar, N. Mir. *Polyhedron*, **27**, 3514 (2008).
[33] A.E. Berkowitz, R.H. Kodama, S.A. Makhlouf, F.T. Parker, F.E. Spada, E.J. McNiff Jr, S. Foner. *J. Magn. Magn. Mater.*, **196**, 591 (1999).
[34] C. Parada, E. Moran. *Chem. Mater.*, **18**, 2719 (2006).